Multimodal Optimization for the Trajectory Planning of Railway Vehicles

Lukas Pröhl
Chair of Mechatronics
University of Rostock
Rostock, Germany
Lukas.Proehl@uni-rostock.de

Harald Aschemann
Chair of Mechatronics
University of Rostock
Rostock, Germany
Harald.Aschemann@uni-rostock.de

***Abstract*—This paper deals with the optimization of velocity trajectories for railway vehicles w.r.t. the total energy consumption between two successive stops. Based on four principle operating modes – acceleration, cruising, coasting, and braking – energy-optimal trajectories are computed by optimizing the sequence of operating modes as well as the corresponding switching points. The optimization involves two consecutive steps: As a basic technique in the first step, a multimodal optimization, namely the Firefly Algorithm (FFA), is utilized to determine the boundaries defined by the timetable request regarding both time and position constraints. In a second step, the energy-optimal solution will be determined within the remaining parameter space reduced by the first step. The advantages of this approach are pointed out by detailed simulation results.**

***Index Terms*— Multimodal optimization, firefly algorithm, energy-optimal trajectory planing, simulation of railway vehicles**

I. Introduction

The trajectory planning for railway applications strongly profits from the previous knowledge about the duty cycles and their characteristics. Whereas road-based traffic applications have to deal with a lot of uncertainties (e.g. unscheduled stops, traffic jams or unknown routes) that affect the driving style, the conditions for railway traffic are in most cases known in advance – like distances, arrival and departure times, speed limits, traffic stops, as well as altitude and tunnel profiles. Based on this previous knowledge, the scheduled time reserve between a time-optimal trajectory (all-out trajectory) and the required timetable may be utilized to optimize the driving style with regard to several objectives such as the reduction of mechanical wear, the reduction of regionally noise pollution or – as the main objective in the current paper – the lowering of the energy consumption.

This energy-optimized driving strategy can be implemented in real-train operations either in the form of a driver advisory system (DAS) or for an automatic train operation (ATO). As an intelligent driving style reduces both the total energy consumption and CO_2 emissions, such a strategy leads both to economic and to environmental benefits.

In the past, a lot of approaches for optimizing the driving style of railway vehicles have been published. Representing a very common technique for this kind of application, dynamic programming was applied in several publications like [1] and [2]. Further contributions like [3] and [4] investigated model-based approaches, which included a combination of a model-based heuristic for the trajectory planning as well as proper optimization techniques to parametrize this heuristic. It is based on the assumption that the energy-optimal trajectory consists of four driving modes – namely acceleration, coasting, cruising and braking. Like in [3], [4] and [5], the switchings between the driving modes are implemented by a trajectory planning module. For an energy-optimal trajectory planning, the switching-points haves to be optimized in order to find a trade-off between the avoidance of high velocities (avoidance of high aerodynamic resistance forces) on the one hand and the maximisation of the duration of coasting (no active propulsion) on the other hand. Accordingly, two parameters are introduced, defining the maximum velocity as well as the length of the coasting phase, that represent the optimization parameters of the trajectory planning problem. These two parameters as well as the functionality of the trajectory planning module are elaborated in more detail in Sect. III.

In [5], the energy-optimal setting for these two parameters is determined in one optimization step only – by defining an objective function that accounts for the total energy consumption and includes additional penalty functions addressing given time and position constraints of the timetable. As the resulting optimization problem may take a non-convex form and as the calculation of gradient information w.r.t. the objective function may become difficult or even impossible due to discontinuities, a particle swarm optimization (PSO) according to [6] is envisaged. However, a high number of particles and iterations must be accepted in order to calculate the optimal solution. This results in a high number of simulations and a corresponding high calculation effort.

The main contributions of this paper can be stated as follows:

- The new two-step optimization approach presented in this paper allows for a significant reduction of the number of simulations.
- It enables the use of a detailed simulation model in practice-relevant tasks.
- It leads to a reduced calculation effort by keeping the high accuracy of the result.

The presented optimization approach is characterised by two

978-1-7281-6929-3/20/$31.00 ©2020 IEEE

consecutive steps, see Fig. 1.

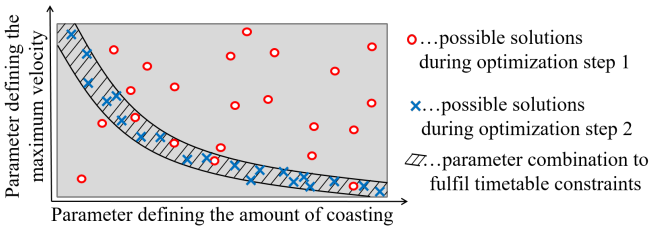

Figure 1. Optimization process with two consecutive steps.

In the first step, the boundaries of feasible solutions, reflecting both position and time constraints of a given timetable, are determined. For this step, a simple simulation model covering the mechanical characteristics of the train only, see Sect. II, is employed. To implement this first optimization step, an objective function is defined that comprises only the penalty terms w.r.t. the constraints. As a result, this objective function is characterised by a flat region (with vanishing gradients) within the non-penalized search space. To find the boundaries of this specific objective function, a multimodal optimization approach is used. Here, a slightly modified firefly algorithm according to [7] is chosen. More details regarding the set-up of this objective function as well as an approach for the optimization of the flat objective function is presented in Sect. IV.

In the second optimization step, the energy-optimal velocity profile is determined by taking advantage of the heavily reduced search space. For this purpose, a detailed simulation model is derived in Sect. II to calculate the energy consumption for a specific track and train characteristic.

The corresponding simulation results are summarized and assessed in Sect. V, whereas Sect. VI concludes the paper and gives an outlook on future work.

II. Model of the Railway Traction Chain

The presented work utilizes a single-train simulation model, which was developed in the EU-founded project [8]. Within the scope of [8], the simulation model was verified by industrial partners throughout the railway sector, see [9].

In this paper, the traction chain simulation model for an electrically driven railway vehicle with an AC power supply is considered, see Fig. 2. The presented optimization approach, however, is not limited to this scenario but is applicable to alternative traction chain characteristics, including trains with an internal combustion engine, hybrid trains or fuel-cell powered traction chains.

Here, the considered simulation model is implemented in the form of a backward simulation, an inverse system model that is based on a block structure that reflects the reverse direction of the physical power flow from the output to the input. Based on a desired velocity profile, a power profile for every single component as well as a total energy consumption at the energy source – here, the catenary – can be calculated. The determination of a proper desired velocity profile is the main objective of the trajectory planning module, which is the topic of Sect. III.

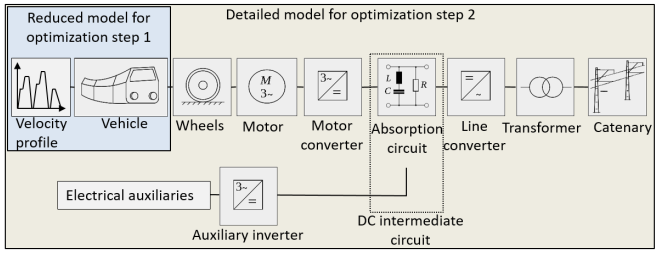

Figure 2. Detailed simulation model of an electrical driven railway vehicle with AC power supply.

As a detailed description of the simulation model can be already already in [5] and [10], only a short summary of the simulation model is given below:

As indicated in Fig. 2, the evaluation of the first optimization step requires only the mechanical properties of the vehicle. The equation of motion, i.e., the differential equation for the vehicle velocity $v(t)$, is given by

$$k_{rot} M \dot{v} = F_{wheel} - \underbrace{\left(c_0 + c_1 v + c_2 v^2\right)}_{F_{res}} - \underbrace{M sin(\gamma) g}_{F_{inc}}. \qquad (1)$$

Here, M denotes the total mass of the vehicle, k_{rot} is a factor accounting for the additional rotary masses, F_{wheel} stands for the force at the wheel, whereas the three coefficients c_0, c_1, and c_2 represent the driving resistance F_{res} described according to the equation of Davis. Moreover, the inclination γ characterizes the inclination force F_{inc}.

The detailed simulation model of the total traction chain, however, is evaluated for the second optimization step as an accurate value for the total energy consumption is desired. The requirement to track the desired velocity profile, in compliance with the mechanical properties of the vehicle, leads to a total power request at the wheel P_{wheel}. The energy losses of the included electrical traction components – motor, motor converter, absorption circuit, line converter, transformer, auxiliary converter – are determined by the evaluation of efficiency maps and idle loss characteristics. In addition to the energy losses of the traction components, the ones of the auxiliaries are considered as well. Here, auxiliary power is required among others for the power profile for the HVAC systems (heating, ventilation and air conditioning), the power request for electrical on-board devices as well as the cooling power profile for the traction components.

III. Operating Strategy of the Trajectory Planning Module

The heuristic employed in the trajectory planning module was elaborated in previous work, see [3] and [5]. For the sake of completeness and to facilitate the understanding, the basic pillars of this heuristic are briefly summarized in the sequel.

To determine the optimal driving strategy, the proposed approach uses four basic driving modes, namely:

- Acceleration – limited by the maximum traction effort and the passenger comfort,
- Cruising – motion at a constant velocity level (no acceleration),
- Coasting – motion without active traction or braking at the wheels,
- Braking – limited by the maximum braking effort as well as the passenger comfort.

The vehicle motion during this four modes can be simulated using the equation of motion according to (1). Here, further physical constraints are taken into account, in particular the maximum traction effort, which is defined by the torque/speed characteristic of the traction motors, and a maximum admissible acceleration to guarantee passenger comfort, see [10].
Fig. 3 shows an exemplary trajectory profile consisting of a combination of all these different driving modes. As indicated in Fig. 3, the switching points between the driving modes define the individual velocity profile. The switching conditions are implemented within the trajectory planning module and are discussed in the sequel.

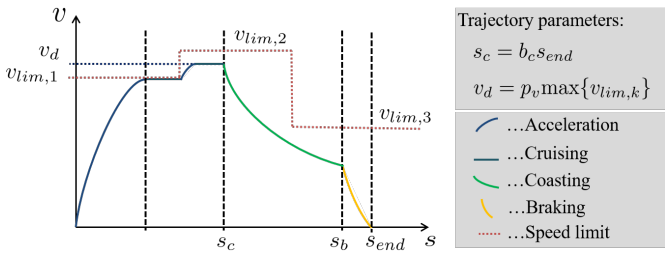

Figure 3. Exemplary trajectory profile based on four characteristic driving modes.

As already mentioned, the optimal location of the switching points corresponds to a trade-off between the maximum velocity and the amount of coasting. Therefore, two trajectory parameters b_c and p_v are introduced. The parameter b_c defines the distance s_c, where the coasting mode will be activated. Given the fixed distance s_{end} towards the next station, the coasting point is calculated as follows

$$s_c = b_c s_{end} \text{ with } b_c \in [b_{c,min} > 0;\ b_{c,max} < 1]\,. \qquad (2)$$

The desired maximum velocity v_d of the travel segment is given by

$$v_d = p_v \max\left\{v_{lim,k}\right\} \text{ with } p_v \in [p_{v,min} > 0;\ 1]\,. \qquad (3)$$

Here, the various segment-specific speed limits are denoted by $v_{lim,k}$, whereas p_v serves as the second optimization parameter of the desired trajectory. A simple example explaining the impact of the two trajectory parameters p_v and b_c is illustrated in Fig. 3.
The braking distance s_b denotes the maximum distance possible to initialize braking in order to still meet given distance constraints for the next stop or the next speed limit. This point is determined by an evaluation of the equation of motion (1) in backward-time direction using the maximum braking effort available.
With this parametrisation of the trajectory planner, the switching conditions for changing the driving state are defined. The trajectory always starts with the acceleration mode, followed by a sequence of other driving modes that are activated as soon as one of the switching conditions I,…, VI is fulfilled and enforces a new driving state. These switching conditions are chosen as follows:

I: $(v = v_d) \vee (v = v_{lim})$
II: $(v < v_d) \wedge (v < v_{lim})$
III: $(v = v_b) \vee (v > 0)$
IV: $(s \geq s_c)$
V: $(s < s_c)$
VI: $(s \geq s_b) \wedge (v > v_b)$

Consequently, the trajectory planning module is capable of creating a proper velocity profile, utilizing the switching strategy as depicted in Fig. 4.

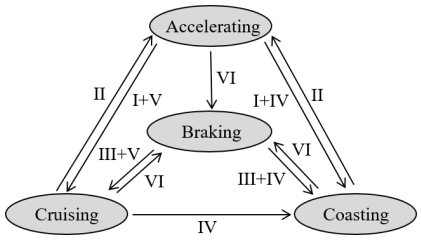

Figure 4. Structure and functionality of the trajectory planning module.

This functionality of the trajectory planning module allows for several alternative trajectory modes – with different character and style. To illustrate this variety, a simple example with only one speed limit is presented in Fig. 5.

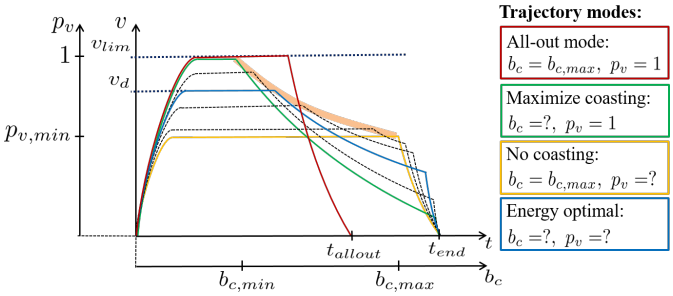

Figure 5. Trajectory modes based on different driving styles.

Here, the red line represents the time-optimal solution, which is denoted as all-out mode. The time-optimal profile includes no coasting and fully exploits the maximum speed limit. Hence, it is characterised by the parameter combination $p_v = 1$ and $b_c = 1$. The presentation of the all-out profile is included only for the purpose of expressing the functionality of the trajectory planning approach. However, it does not meet the desired arrival time of the timetable, it arrives too early, and will not be part of the following discussion.

In contrast, all other velocity profiles fulfil the timetable. For instance, a fixed parameter $p_v = 1$ defines the green curve, which represents a characteristic profile for maximising the amount of coasting (utilizing maximum speed limits). Here, only the parameter b_c has to be determined in order to meet the timetable constraints. In this work, a bisection technique is employed for this purpose. In analogy, the yellow curve represents another important driving profile, which corresponds to a trajectory without coasting. Here, the parameter $b_c = b_{c,max}$ is fixed, which excludes the possibility of coasting. To fulfil the timetable requirements, the maximum velocity has to be reduced. Again, a bisection algorithm is used to determine the corresponding parameter p_v defining the admissible maximum velocity.
In Fig. 5, the bold orange curve indicates all parameter combinations that allow for meeting the timetable. This curve emphasizes the solutions of optimization step I. The determination of the energy-optimal solution, represented by the blue curve, within this reduced parameter set is the objective of optimization step II.

IV. Optimization of a Flat Objective Function Representing the Constraints

This section deals with the determination of flat regions in the surface described by the objective function. Here, a flat region is defined as a part of the objective function characterized by a vanishing gradient. The objective is to determine the boundaries of these flat regions. The presented approach takes advantage of the firefly algorithm (FFA), cf. [7], which is capable of solving multimodal optimization problems. A short summary of the FFA as well as a demonstration example are provided below.

A. Summary of Firefly Algorithm

The firefly algorithm belongs to the class of particle optimization. As all particle optimization techniques, it does not require any gradient information of the considered objective function. Additionally, the firefly algorithm is capable of finding multiple optimal solutions, including local solutions as well. This property is beneficial because it allows for a higher flexibility if the globally optimal solution is not applicable for some reason.
As the name indicates, the FFA is inspired by the swarm behaviour of fireflies in their real natural environment. The light emission of the fireflies serves for attracting both potential pray as well as mating partners. For the firefly algorithm, the analogy between the light intensity and the attractiveness is exploited. Here, maximising the light intensity corresponds to optimizing the objective function $J(\underline{x})$.
In the sequel, the position of the i-th particle within a 2-dimensional search space is denoted by $\underline{x}_i = [x_i \;\; y_i]^T$. The attractiveness of a single particle i w.r.t. another particle j is described by

$$\beta(r) = \beta_0 e^{-\gamma r_{ij}^2}, \tag{4}$$

where the Euclidean distance r_{ij} between the two particles is given by

$$r_{ij} = \sqrt{(x_i - x_j)^2 + (y_i - y_j)^2}\ . \tag{5}$$

The coefficient γ denotes an absorption factor in analogy to the absorption of light emitted by the fireflies. The attractiveness of a firefly for $r = 0$ is defined as β_0. Please note that the absorption factor represents a parameter to be adjusted according to the width of the given search space.
Based on this definition of the attractiveness and the additional assumption that the motion of the firefly is only motivated by fireflies with higher attractivity, the motion of particle i is governed by

$$\underline{x}_{i+1} = \underline{x}_i + \beta(r) \cdot \left(\underline{x}_j - \underline{x}_i\right) + \alpha \cdot \mathrm{rand}([-0.5, 0.5]). \tag{6}$$

Here, the coefficient α characterises the effect of the random proper motion. The expression $\mathrm{rand}([-0.5, 0.5])$ denotes a randomly distributed number in the range of $[-0.5, 0,5]$. Typically, there is an underlying heuristic to increase the randomness factor α during the progression of the iterations.

B. Demonstration Examples for Determining Boundaries by Multimodal Optimization

To express the capability of optimizing a multimodal objective function, including a flat region, this section demonstrates the application of the FFA to a simple example:
The considered objective function is given by

$$J'(x,y) = \begin{cases} 2 & \text{if } (x+2)^2 + (y+4)^2 < 1, \\ e^{(-(x-4)^2-(y-4)^2)} \ldots & \\ +\ e^{(-(x+4)^2-(y-4)^2)} \ldots & \\ +2e^{(-(x+1)^2-(y+4)^2)} \ldots & \\ +2e^{(-(x-1)^2-(y-1)^2)} & \text{else.} \end{cases}$$

Here, a flat region exists in addition to three other relative maxima. The simulation result for 100 particles after the completion of 50 iterations is depicted in Fig. 6.

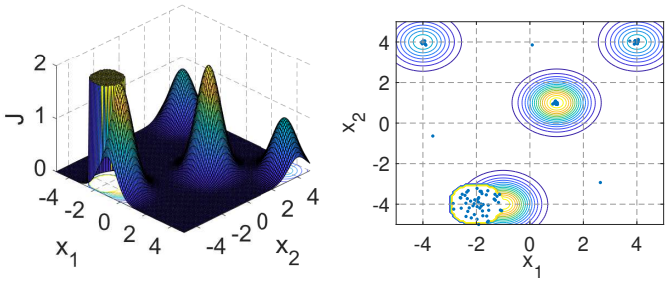

(a) Demonstration function $J'(x,y)$. (b) Particle distribution after 50 iterations for demonstration function $J'(x,y)$.

Figure 6. Application of FFA for an objective function with a flat region.

As visible in Fig. 6 (b), the algorithm is capable of determining all optimal regions. Within the flat region, the particles are evenly distributed. By an proper geometrical evaluation of the

particle position at the end of the optimization process, the boundaries of the flat region can be determined. Please note that the algorithm can be easily applied for any minimisation task as well by evaluating

$$\min_{\underline{x}}\left(J(\underline{x})\right) = \max_{\underline{x}}\left(-J(\underline{x})\right). \tag{7}$$

V. Application to a Railway Scenario

The objective of this section is the application of the optimization strategy presented above to a selected railway scenario. A set of generic railway architectures and proper parametrized traction chains are developed in [8] and [11]. In this paper, a high-speed train service is chosen. This train service is characterised by a high vehicle speed over a long distance. Especially for this service, an energy-optimal trajectory planing offers a huge potential in terms of energy saving. The reason is that the trade-off between the avoidance of high aerodynamic drag and the possible coasting is distinct. For the presented railway application, a high-speed train with a maximum speed of 300 km/h is considered, approaching 3 different stations (start, intermediate and final) and covering a total distance of 300 km.
Within this section, the two steps of the optimization process are applied for this specific scenario:

Step I:
Determination of Boundaries Defined by the Timetable
The objective of the first step is the determination of the boundaries taking into account the given time and position constraints of the timetable. The desired departure and arrival times t_0, t_f as well as the corresponding positions s_0, s_f are utilized to define the following penalty functions

$$J_s = \begin{cases} \left(s_{dr} - (s_f - s_0)\right)^2 & \text{if } \left|s_{dr} - (s_f - s_0)\right| > \Delta s, \\ 0 & \text{else}, \end{cases} \tag{8}$$

and

$$J_t = \begin{cases} \left(t_{dr} - (t_f - t_0)\right)^2 & \text{if } \left|t_{dr} - (t_f - t_0)\right| > \Delta s, \\ 0 & \text{else}. \end{cases} \tag{9}$$

Here, Δt and Δs are admissible time and position tolerances for the arrival at the station. These penalty functions assess the calculated driving time t_{dr} as well as driving distance s_{dr}, which are determined using the mechanical model of the train, see Fig. 2.
As a result, the overall cost function for the first optimization step is chosen as

$$J_I = \begin{cases} J_t + J_s & \text{if } J_t \neq 0 \ \vee \ J_s \neq 0, \\ J_0 & \text{else}. \end{cases} \tag{10}$$

The term $J_0 \leq 0$ characterises the flat region of the objective function, where no active constraints are applied. The solutions of the optimization problem for step I can now be stated as

$$\left[p_v^I,\, b_c^I\right] = \arg\left\{\min_{p_v, b_c}\{J_I(p_v, b_c)\}\right\}. \tag{11}$$

The evaluation of the FFA for this objective function leads to a particle distribution that represents the parameter space where all the timetable constraints are fulfilled.

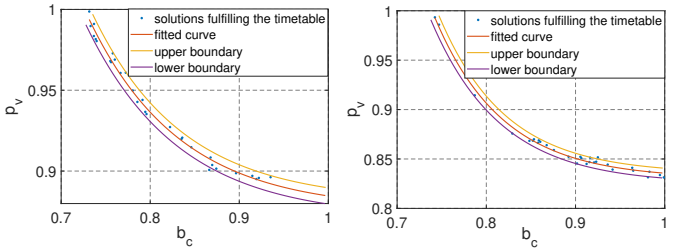

(a) Result of first optimization step (FFA-application) for travel from station A to B.

(b) Result of first optimization step (FFA-application) for travel from station B to C.

Figure 7. Application of the first optimization step to the high-speed scenario.

Fig. 7 depicts the resulting particle distribution as well as a fitted curve representing averaged solutions, which are determined by utilizing common fitting techniques. Additionally, it is possible to determine upper as well as lower bounds to include the resulting solutions and define an interval for the permitted parameters. Note that the width of this interval is correlated with the admissible time and position tolerances Δt and Δs.

Step II:
Determination of the Energy-Optimal Solution
Thanks to step I, the parameter space is limited to a set of feasible parameters. Now, the objective of step II is the determination of the energy-optimal solution. Hence, the objective function for the second step is related to the total net-energy of the train

$$J_{II} = E_{total} = E_{cons} - E_{rec}\ . \tag{12}$$

Here, the total net-energy is the sum of the energy taken from the net E_{cons} and the recuperated one E_{rec}. For this objective, the complete traction chain of the train (see Fig. 2) has to be evaluated to calculate the total energy consumption. Hence, the corresponding solutions for the optimization problem of the second step can be stated as

$$\left[p_v^{II},\ b_c^{II}\right] = \arg\left\{\min_{p_v \in p_v^I, b_c \in b_c^I}\{J_{II}(p_v, b_c)\}\right\}. \tag{13}$$

Also for this optimization problem, gradient information is not available. Instead, several gradient-free optimization techniques may be applied. For the illustration of the applied scenario, selected energy consumptions for the average characteristic as well as for the upper and lower boundary are shown in Fig. 7.
As depicted in Fig. 7, the energy consumption for the lower and higher boundary is decreased and increased in comparison to the averaged solutions, respectively. This effect is caused by the definition of the admissible time and distance tolerances Δt, Δs – the lower boundary, e.g., is defined by the longest admissible travel time ($t_{max} = (t_f - t_0) + \Delta t$) in combination with

the shortest permissible travel distance ($s_{min} = (s_f - s_0) - \Delta s$), which obviously leads to a decreased energy consumption. For the upper boundary, this correlation is applicable vice versa.

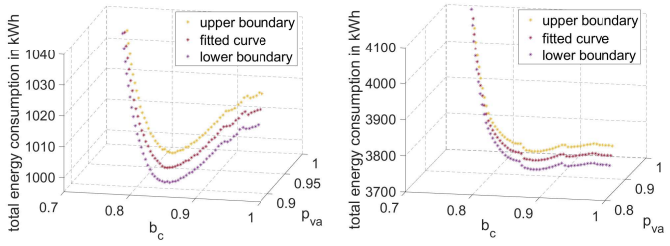

(a) Total energy consumption for the travel segment from station A to B.

(b) Total energy consumption for the travel segment from station A to B.

Figure 8. Total energy consumption for highspeed scenario.

Hence, the average curve can be considered as the solution with minimum deviations regarding the desired timetable. In Fig. 9, the resulting speed profiles for the highest and lowest energy consumption for the mean characteristic are depicted.

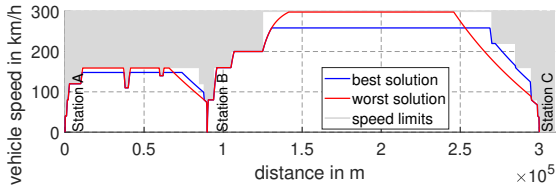

Figure 9. Comparison of the worst and best velocity profile according to the energy-consumption.

It becomes obvious that the worst solution is related to the approach of maximising the amount of coasting, which is, however, a standard approach in railway operation. The optimal solution allows for a significant reduction in the energy consumption and clearly points out the benefits of this optimization study.

The total energy consumptions for both scenarios are comprised in Tab. I.

Segment	Energy consumption in kWh		Total energy savings in kWh	Total energy savings in %
	Maximum coasting	Optimized trajectory		
Station A–B	1033	1000	33	≈ 3.2
Station B–C	4070	3766	304	≈ 7.5
Total net energy	5103	4766	337	≈ 6.6

Table I
ENERGY SAVINGS DUE TO THE ENERGY-OPTIMAL DRIVING STYLE.

VI. CONCLUSIONS AND OUTLOOK ON FUTURE RESEARCH

In this paper, an optimization regarding energy-optimal velocity profiles for railway vehicles is presented. As one pillar for the calculation of the velocity profiles, a heuristic trajectory planning module is proposed. This module defines switching points between typical driving modes. As a second pillar, a detailed simulation model of the complete traction chain for the application scenario is presented as well.

A two-step optimization approach was presented for determining the energy-optimal switching points for the driving modes: In the first step, a reduced-order simulation model was evaluated to determine boundaries caused by time and position constraints according to the desired timetable. For this purpose, a proper objective function was defined, where the admissible solutions are located within a flat region with vanishing gradients. To calculate the boundary of this flat region, a firefly algorithm (FFA) was successfully applied.

In the second optimization step, the energy-optimal solution is determined within the reduced parameter space by evaluating the total energy consumption with the simulation structure of the total traction chain.

In future research, the investigation of further operating scenarios is planned. Especially, the consideration of altitude profiles is of great interest, because the benefit of applying energy-optimal driving strategies is even more distinct. The reason is that the consideration of an altitude profile allows for additional driving modes (e.g. acceleration/deceleration without any traction power at the wheel during downhill/uphill sections).

Moreover, a holistic optimization of the driving style in combination with further operating strategies – strategies for the energy storage system (ESS) , component switch-offs during low load phases, adjustments of the auxiliary load according to the driving mode – is of great interest.

REFERENCES

[1] P. Howlett. The optimal control of a train. In *Annals of Operations Research*, volume 98 of *1-4*, pages 65–87, 2000.

[2] R. Franke, P. Terwiesch, and M. Meyer. An algorithm for the optimal control of the driving of trains. In *Proceedings of the 39th IEEE Conference on Decision and Control*. IEEE, 2000.

[3] M. Leska, R. Prabel, A. Rauh, and H. Aschemann. Simulation and optimization of the longitudinal dynamics of parallel hybrid railway vehicles. In G. Tarnai E. Schnieder, editor, *FORMS/FORMAT*, volume 281, pages 155–164. Springer-Verlag, 2010.

[4] M. Leska, T. Grüning, H. Aschemann, and A. Rauh. Optimization of the longitudinal dynamics of parallel hybrid railway vehicles. *IEEE Multi-Conference on Systems and Control*, 2012.

[5] L. Pröhl and H. Aschemann. Energy optimal trajectory planning for electrically driven railway vehicles with particle swarm optimization. In *2019 IEEE 15th International Conference on Control and Automation (ICCA)*, pages 423–428, July 2019.

[6] J. Kennedy and R. Eberhart. Particle swarm optimization. In *Proceedings of ICNN'95 - International Conference on Neural Networks*. IEEE, 1995.

[7] X.S. Yang. Firefly algorithms for multimodal optimization. In Osamu Watanabe and Thomas Zeugmann, editors, *Stochastic Algorithms: Foundations and Applications*, pages 169–178, Berlin, Heidelberg, 2009. Springer Berlin Heidelberg.

[8] Shift2Rail project OPEUS. Modelling and strategies for the assessment and OPtimisation of Energy USage aspects of rail innovation, project reference: 730827. http://www.opeus-project.eu/, 2019.

[9] Holger Dittus, Henry Völker, Lukas Pröhl, Harald Aschemann, Stefan Heibl, and Roberto Palacin. Energy assessment in shift2rail european rail research project. In *12th World Congress on Railway Research - Congress Proceedings WCRR 2019*, 2019.

[10] Shift2Rail project OPEUS. OPEUS Simulation Package, OPEUS Deliverable Report D2.1. Shift2Rail website - OPEUS project, October 2017.

[11] J. Ernst. FINE1 Deliverable D3.1 - Energy Baseline. *Shift2Rail project FINE1, Future Improvement for Energy and Noise, project reference: 730818*, 2018.